Journal of Molecular Graphics and Modelling 37 (2012) 27–38

Contents lists available at SciVerse ScienceDirect

Journal of Molecular Graphics and Modelling

journal homepage: www.elsevier.com/locate/JMGM

Dual inhibition of chaperoning process by taxifolin: Molecular dynamics simulation study

Sharad Verma[a], Amit Singh[b], Abha Mishra[a,*]

[a] School of Biochemical Engineering, Institute of Technology, Banaras Hindu University, Varanasi 221005, India
[b] Department of Pharmacology, Institute of Medical Sciences, Banaras Hindu University, Varanasi 221005, India

ARTICLE INFO

Article history:
Received 9 December 2011
Received in revised form 4 April 2012
Accepted 17 April 2012
Available online 23 April 2012

Keywords:
Hsp90
Cdc37
Chaperone
Taxifolin

ABSTRACT

Hsp90 (heat shock protein 90), a molecular chaperone, stabilizes more than 200 mutated and over expressed oncogenic proteins in cancer development. Cdc37 (cell division cycle protein 37), a co-chaperone of Hsp90, has been found to facilitate the maturation of protein kinases by acting as an adaptor and load these kinases onto the Hsp90 complex. Taxifolin (a natural phytochemical) was found to bind at ATP-binding site of Hsp90 and stabilized the inactive "open" or "lid-up" conformation as evidenced by molecular dynamic simulation. Furthermore, taxifolin was found to bind to interface of Hsp90 and Cdc37 complex and disrupt the interaction of residues of both proteins which were essential for the formation of active super-chaperone complex. Thus, taxifolin was found to act as an inhibitor of chaperoning process and may play a potential role in the cancer chemotherapeutics.

1. Introduction

Molecular chaperones perform correct folding of a number of proteins inside the cell, however, also play a significant role in cancer proliferation. Hsp90 (heat shock protein 90) was first characterized with regard to role of molecular chaperones in cancer [1]. Hsp90 stabilizes a wide range of mutated and over expressed oncogenic proteins [2,3]. Hsp90 expression is constitutive in tumor cells at 2–10-fold higher levels compared to normal cells [4,5]. More than 200 proteins molecules folded by Hsp90 in their stabilized and active conformation state [6]. Protein kinases are known to be involved in cell proliferation and may cause cancer when deregulated. Protein kinases depend on Hsp90 for proper folding to be functional. Hsp90 requires a series of co-chaperones to form functional super-chaperone complex. These co-chaperones regulate the chaperoning process by association and dissociation with Hsp90. Cdc37 (cell division cycle protein 37) is a co-chaperone of Hsp90 has been characterized as a protein kinase recruiting subunit of the Hsp90 machinery [7]. Cdc37 facilitates the maturation of these kinases by acting as an adaptor and load kinases "onto" the Hsp90 complex [2,8–10]. Hsp90 possesses ATP-binding pocket which is distinct from the ATP-binding cleft of protein kinases [11]. The Hsp90 structure consists of three domains: (1) an amino terminal region (N terminal domain, NTD) that for ATP binding, (2) a middle region (M domain) that provides interaction sites for client proteins and co-chaperones to form an active ATPase and (3) a carboxy-terminal region (C domain) that contains a dimerization motif [12–14]. Chaperone function necessarily requires dimerization of two Hsp90 protomers through their C domains [15,16]. There are two main ways to modulate chaperoning process: (1) inhibition of ATPase activity of Hsp90 which is essential for dimerization and successful performance of chaperone cycle, (2) prevention of proper association of co-chaperones with Hsp90 which is mandatory process for recruitment of client proteins. Taxifolin is a one of the principal active component of plants such as *Larix gmelini* [17], *Silybum marianum*, *Acacia* sp., *Rhododendron* sp. Taxifolin (2-(3,4-dihydroxyphenyl)-2,3-dihydro-3,5,7-trihydroxy-4H-benzopyran-4-one) is a dihydroflavonol with distinguished antioxidant activity compared to other antioxidants [18,19]. It has free radical scavenging property, can improve the impermeability of capillary vessels and recover their elasticity effectively. It is not embryotoxic and does not lead to malformations, hyper susceptibility or mutations [20].

In the present study effort was made to evaluate the effect of taxifolin on chaperon cycle in reference to Hsp90 apo form and Hsp90–cdc37 complex.

2. Computational methods

2.1. Molecular docking

AutoDock 4.0 suite was used as molecular-docking tool in order to carry out the docking simulations. Pdb id 3K97 and 3K5B, obtained from RCSB protein data bank, were used as initial structure

* Corresponding author. Tel.: +91 5422307070.
E-mail address: abham.bce@itbhu.ac.in (A. Mishra).

1093-3263/$ – see front matter © 2012 Elsevier Inc. All rights reserved.
http://dx.doi.org/10.1016/j.jmgm.2012.04.004

for Hsp90 NTD apo form and Hsp90–cdc37 complex respectively. The structure of ligand taxifolin was generated from smile strings followed by energy minimization. All the heteroatom was removed except Mg ion. Hydrogen atoms were added to protein crystal structures using autodock program while all non polar hydrogen atoms were merged. Six bonds were made rotatable for the taxifolin. Lamarckian genetic algorithm was used as a search parameter which is based on adaptive local search. Short range van der Waals and electrostatic interactions, hydrogen bonding, entropy losses were included for energy based autodock scoring function [21,22]. The Lamarckian GA parameters used in the study were numbers of run, 30; population size, 150; maximum number of eval; 25,000,000, number of generation; 27,000, rate of gene mutation; 0.02 and rate of cross over; 0.8. Blind docking was carried out using grid size 126, 126 and 126 along the *X*, *Y* and *Z*-axes with 0.375 Å spacing. RMS cluster tolerance was set to 2.0 Å. Semi-flexible docking was performed which includes a flexible ligand and a rigid receptor. All the protein and ligand structural images were generated using PyMol [23].

2.2. Molecular dynamic simulation in water

MD simulation of the complex was carried out with the GROMACS 4.5.4 package using the GROMOS96 43a1 force field [24,25]. The lowest binding energy (most negative) docking conformation generated by Autodock was taken as initial conformation for MD simulation. The topology parameters of proteins were created by using the Gromacs program. The topology parameters of taxifolin were built by the Dundee PRODRG server [26]. The complex was immersed in an octahedron box of simple point charge (SPC) water molecules [27,28]. The solvated system (Hsp90, taxifolin and water) was neutralized by adding 8 Na ions, and 7 Na ions in case of Hsp90 NTD-taxifolin and Hsp90–cdc37–taxifolin complex respectively. To release conflicting contacts, energy minimization was performed using the steepest descent method of 10,000 steps followed by the conjugate gradient method for 10,000 steps. MD simulation studies consist of equilibration and production phases. To equilibrate the system, the solute (protein, counterions, and taxifolin) were subjected to the position-restrained dynamics simulation (NVT and NPT) at 300 K for 300 ps. Finally, the full system was subjected to MD production run at 300 K temperature and 1 bar pressure for 10,000 ps. For analysis, the atom coordinates were recorded at every 0.5 ps during the MD simulation.

3. Results and discussion

3.1. Interaction of taxifolin with Hsp90

Docking studies revealed that taxifolin was found to bind at ATP-binding site of Hsp90 with lowest binding energy of −31.08 kJ/mol. Free energy of binding was calculated as a sum of four energy terms of intermolecular energy (van der Waals, hydrogen bond, desolvation and electrostatic energy), total internal energy, torsional free energy and unbound system energy. The major interactions shown in the Hsp90-ATP-binding site were important H-bonds with Asn 51, Ser 52, Lys 58, Asp 93 and Gly 97 (Supplementary Fig. 1). The groups involved in H-bonding were hydroxyl (hydrogen donor), and carbonyl (hydrogen acceptor) group of taxifolin and NH (hydrogen donor) and oxygen atoms (hydrogen acceptor) of side chain or backbone of residues.

The Hsp90–taxifolin complex with the binding energy of −31.08 kJ/mol obtained using Autodock was used for carrying out MD simulation. We have analyzed the time dependent behavior of MD trajectories for Hsp90–taxifolin complex including root mean square deviation (RMSD) for all backbone atoms, average

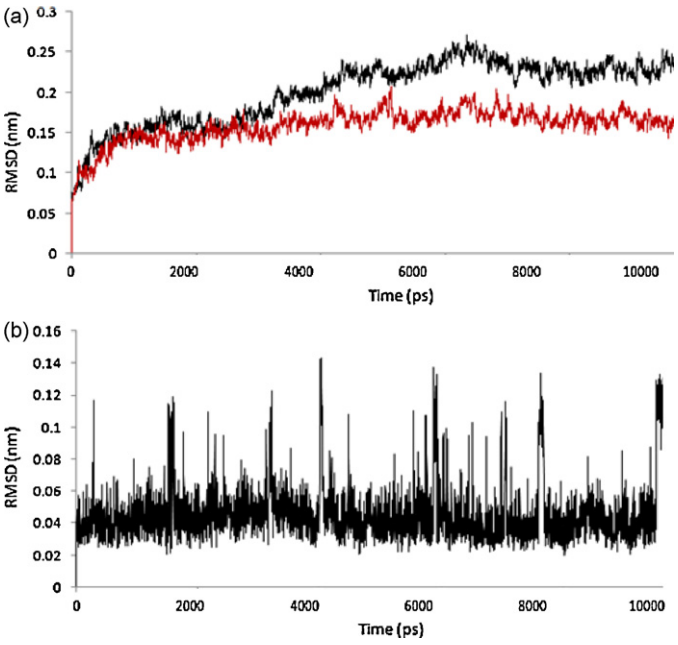

Fig. 1. (a) Plot of root mean square deviation (RMSD) of backbone of Hsp90 unbound (black) and Hsp90–taxifolin complex (red). (b) Plot of root mean square deviation (RMSD) of taxifolin. The trajectories were captured every 0.5 ps until the simulation time reached 10,000 ps. (For interpretation of the references to color in this figure legend, the reader is referred to the web version of this article.)

fluctuations of the residues (RMSF) along with radius of gyration (Rg). RMSD of backbone atoms with respect to the initial conformation was calculated as a function of time to assess the conformational stability of the protein during the simulations. Fig. 1(a) shows that the RMSD profiles were always less than 0.3 nm for the entire simulation which suggested the stability of Hsp90–taxifolin complex. An initial steep rise in the RMSD for the first, ∼1000 ps and subsequently a constant profile was observed for the taxifolin bound Hsp90. Taxifolin unbound form showed slight higher RMSD after ∼3500 ps. These results showed that the trajectories of the MD simulations after equilibrium were reliable for post analyses. RMSD profile of taxifolin showed more or less constant pattern below 0.16 nm with marked fluctuation at different time interval (Fig. 1(b)). Analysis of taxifolin RMSD indicated that taxifolin showed remarkable stability for ATP-binding pocket during MD simulation. To investigate the thermodynamic stability of complex during simulation, potential energy fluctuation was analyzed. The potential energy trajectories were adhered to constant values for the Hsp90–taxifolin complex during the entire simulation length. Number of H-bonds (cut off 0.35 nm) which were formed during MD simulation between taxifolin and Hsp90 also calculated. A variable profile was observed which fluctuate between 0 and 5 with an average value of 1.12 (Fig. 2). Apart from the H-bonds, hydrophobic interactions between taxifolin and binding site residues were also analyzed. 2D plots at the different time of simulation, generated by Discovery studio 3.1 [29]. Fig. 3, revealed that side chain of residue Phe 138 involved in strong π–π interaction with aromatic ring of taxifolin. Taxifolin RMSD along with H-bonding and hydrophobic interaction analyses confirmed the stable interaction of taxifolin at ATP binding site of Hsp90. Radius of gyration (Rg) of Hsp90 and Hsp90–taxifolin complex were analyzed to determine the effect of taxifolin on the folding of Hsp90. Rg value of complexes was found nearly same with continuous up and down during simulation (Fig. 4(a)). To identify the flexible regions of the protein, Root Mean Square Fluctuation (RMSF) of backbone residues from its time averaged position was analyzed. Taxifolin inbound form

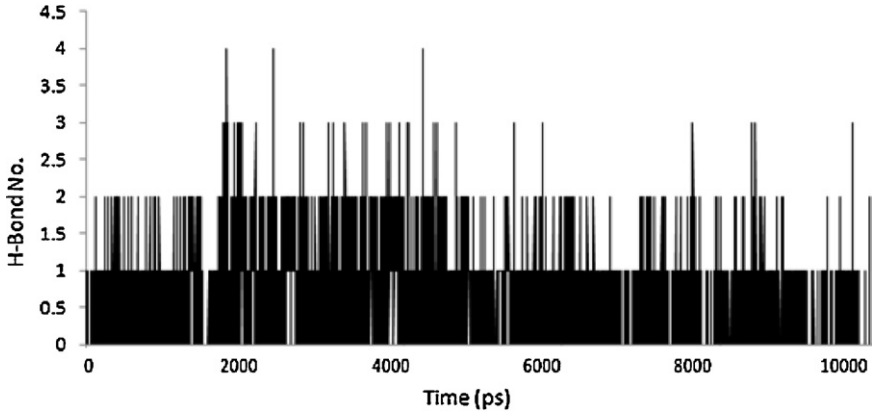

Fig. 2. Number of H-bonds formed between taxifolin and Hsp90 during 10,000 ps MD simulation.

showed markedly higher fluctuations as compared to unbound form (Fig. 4(b)).

Several researchers have worked on targeted suppression of the ATPase activity of Hsp90 with small molecule inhibitors demonstrated anticancer activity in preclinical models and promising safety profile in humans [30–35]. Conformational coupling to the ATPase cycle requires N-terminal domain (NTD) dimerization for ATP hydrolysis and conformational transitions of a segment of the NTD structure known as the "ATP-lid". This segment is composed of two helices with the intervening loop located immediately adjacent to the ATP binding site [13]. The crystal structures of human Hsp90 NTD complexes with ADP (PDB id. 1BYQ) [36] and geldanamycin (a known inhibitor of Hsp90, PDB id. 1YET) [37] have revealed that the "ATP-lid" segment projects out of the N-domain ("open" or "lid-up" conformation) [38,39]. Ali et al. reported the crystal structure of the ATP-bound conformation Hsp90 NTD (PDB id. 2CG9) which

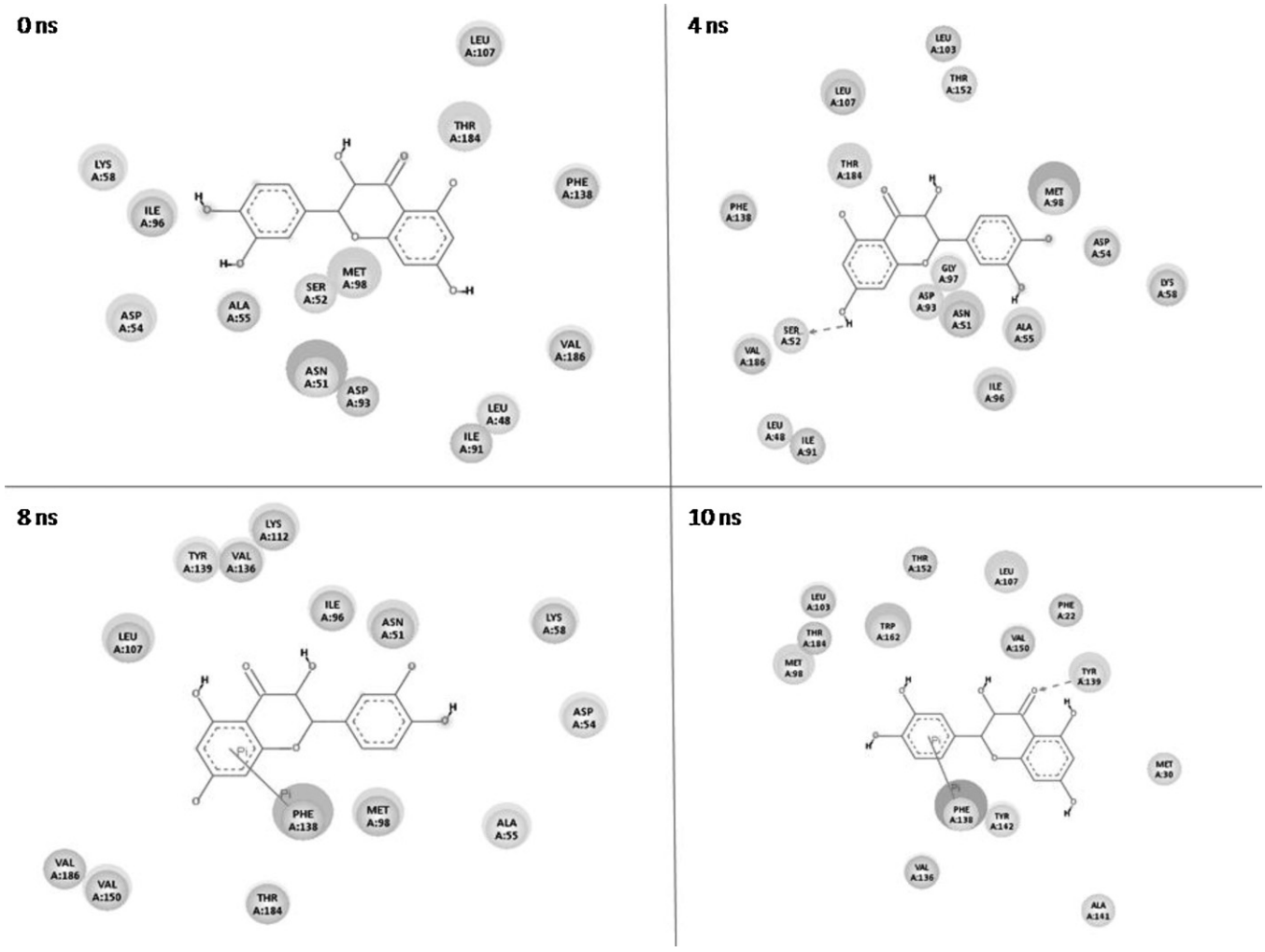

Fig. 3. 2D plots of interaction between taxifolin and Hsp90 at different time interval of MD simulation.

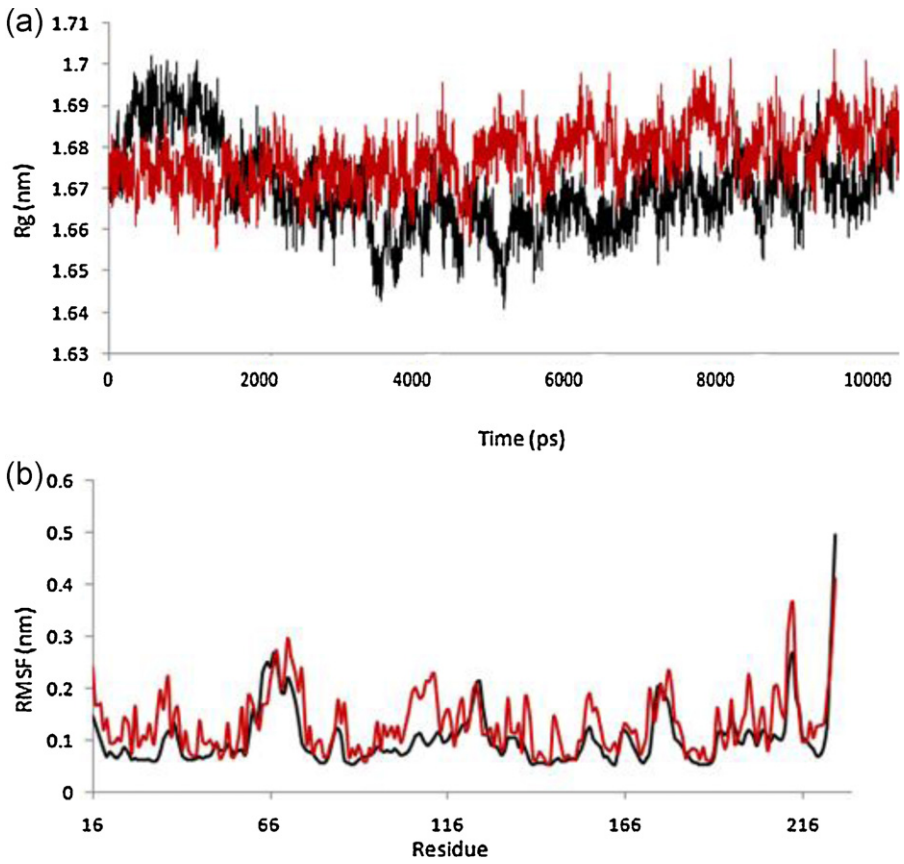

Fig. 4. (a) Radius of gyration of Hsp90 unbound (black) and Hsp90–taxifolin complex (red). (b) RMSF of Hsp90 backbone (black) and Hsp90–taxifolin backbone (red). (For interpretation of the references to color in this figure legend, the reader is referred to the web version of this article.)

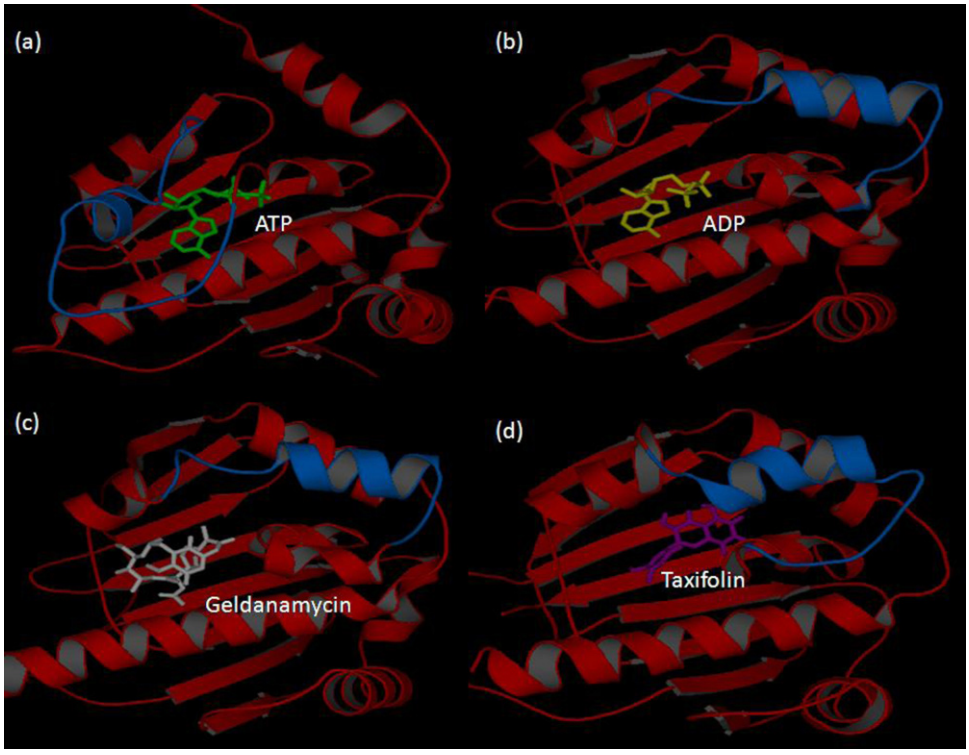

Fig. 5. (a) ATP bound "closed" or "lid-down" conformation of Hsp90 N-terminal domain. (b) ADP bound "open" or "lid-up" conformation of Hsp90 N-terminal domain. (c) Geldanamycin bound "open" or "lid-up" conformation of Hsp90 N-terminal domain. (d) Taxifolin bound "open" or "lid-up" conformation of Hsp90 N-terminal domain after 10,000 ps MD simulation.

showed that the lid segment of Hsp90 can be displaced from its position and folds over the nucleotide pocket to interact with the bound ATP ("closed" or "lid-down" conformation) [13]. Thus the ATPase cycle results in a structurally rigid conformational state of Hsp90 upon ATP binding, whereas on hydrolysis to ADP leads to a more structurally flexible state of Hsp90 [38,11,40]. The conformational transition of the lid segment modulated by the inhibitor binding which stabilizes the open or lid-up conformation [13]. The hydrolysis of ATP to ADP or binding with the active inhibitor leads to more relaxed and nonfunctional state of Hsp90 NTD. It is evident from MD simulation studies that taxifolin stabilized the open lid conformation of Hsp90 NTD. The loop of "ATP-lid" segment was pulled toward the taxifolin. A comparative investigation of ADP, geldanamycin and taxifolin bound Hsp90 NTD revealed the significant similarity in the overall structure (Fig. 5).

3.2. Interaction of taxifolin with Hsp90–cdc37 complex

Hsp90 interacts with multiple co-chaperones to form a superchaperone complex, including Cdc37, Aha1, p23/Sba1, Hop, Hsp70, and Hsp40 [41–43]. Each component in the complex has specific role associated with different types of protein. Cdc37, originally named as p50, was reported as an accessory factor to load the protein kinases to Hsp90 in the Hsp90 superchaperone complex [2,7,44]. Silencing of Cdc37 reduces expression of a number of proteins such as ERBB2, CRAF, CDK4, CDK6, and phosphorylated AKT, which are highly relevant to cancer progression [45]. Thus the involvement of the Hsp90–cdc37 complex in the maturation and activity of oncogenic protein kinases makes the complex, a potential therapeutic target for cancer chemotherapy. Recently, a quinine methide triterpene compound Celastrol was shown to disrupt Hsp90/Cdc37 interaction and exhibited anticancer activity [46,47], which support the potential application of disrupting the protein/protein interaction of the Hsp90–cdc37 complex for cancer therapy. Cdc37 is composed of the following three domains: a 15.5 kDa N-terminal domain (residues 1–127), a 16 kDa middle domain (residues 147–276), and a 10.5 kDa C-terminal domain (residues 283–378) [48,49]. Cdc37 forms a complex with the N terminus of Hsp90 through its middle and C-terminal portions [50,51]. NMR mapping using human N-terminal Hsp90 (residues 18–223) and middle terminal Cdc37 (residues 147–276) fragments further showed a series of residues in the interaction patch, including Ser 113, Lys 116, Ala 117, Glu 120, Ala 121, Ala 124, Ala 126, Met 130, Gln 133, and Phe 134 of Hsp90 and His 161, Met 164, Leu 165, Arg 166, Arg 167, Asp 170, Trp 193, Ala 204, Leu 205, and Gln 208 of Cdc37 [52,53].

To investigate probable role of taxifolin in disruption of the Hsp90–cdc37 interaction, we first examined whether taxifolin could bind residues at the interface of the Hsp90–cdc37 complex. Molecular docking study revealed that taxifolin was interacted with Hsp90–cdc37 interface residues with binding energy of −27.17 kJ/mol. Taxifolin formed H-bond with the residues: His 210 of Hsp90 and Lys 242 of Cdc37. For the confirmation of stability of taxifolin at Hsp90–cdc37 complex interfaces and to study the dynamic changes at Hsp90–cdc37 interface, molecular dynamic simulation was performed. Fig. 6(a) shows that the RMSD profiles of backbone were always less than 0.3 nm for the entire simulation suggest the stability of simulation system. Taxifolin RMSD showed continuous fluctuations up to 0.16 nm throughout the MD simulation which suggests that significant domain movements were involved (Fig. 6(b)). The adherence of the potential energy trajectories to more or less constant values for the Hsp90–cdc37 complex and for the taxifolin docked complexes was observed during the entire simulation length (Fig. 7(a)). The energy values of the taxifolin bound complex were much lowered than that of the Hsp90–cdc37 complex, indicating the thermodynamic stability of the ternary complex [10,54,55]. Number of H-bonds (cut off 0.35 nm) which were formed during MD simulation between taxifolin and Hsp90–cdc37 complex interfaces was also calculated. A variable profile was observed which fluctuate between 0 and 6 with an average value of 1.24 (Fig. 7(b)). 2D plots at the different time of simulation revealed that side chain of residue Tyr 216 of Hsp90 and Lys 242 of Cdc37 involved in π–π and cation–π interaction with aromatic ring of taxifolin respectively (Fig. 8). The simulation length used in this study was found to be enough to allow rearrangement of side chains of the native as well as the drug complexed proteins to find their most stable binding mode. To identify the flexible regions of the protein, RMSF of backbone from its time averaged position was analyzed. The RMSF profile of residue backbone revealed slight higher fluctuation in taxifolin bound complex as compared to unbound form during the course of simulation. This suggests that binding of taxifolin makes backbone more flexible to move. Further, the flexibility of Hsp90 backbone was found more as compared to Cdc37. This might be due to the restriction caused by interaction of taxifolin to Cdc37 (Fig. 9). The RMSF profile of critically required interface residue side chains (involved in complex formation) suggested higher fluctuation in taxifolin bound complex as compared to unbound form throughout MD simulation study (Fig. 10). These results suggested that binding of taxifolin made these residues either structurally unrestricted or disruption of stable interactions at the interface.

3.3. Principal component analysis

Reducing the dimensionality of the data obtained from molecular dynamics simulations can help in identifying configurational space that contains only a few degrees of freedom in which anharmonic motion occurs. Principal components analysis (PCA) is a method that takes the trajectory of a molecular dynamics simulation and extracts the dominant modes in the motion of the molecule [56–60]. These pronounced motions correspond to correlated vibrational modes or collective motions of groups of atoms in normal modes analysis [61]. The overall translational and rotational motions in the MD trajectory were eliminated by a translation to the average geometrical center of the molecule and by least squares fit superimposition "onto" a reference structure [57]. In this approach the most important motions of the protein were extracted from the trajectory by principal component analysis of the Cartesian coordinate covariance matrix, yielding eigenvectors and corresponding eigenvalues. The eigenvectors with the largest associated eigenvalues define the essential subspace in which most of the protein dynamics occurs. The rapid decay in the plot of sorted eigenvalues showed that a few eigenvectors suffice to describe the motions of the Hsp90–cdc37 complex i.e. the protein backbone motion can be described by a few essential modes. Principal components analysis was applied to the backbone atoms in taxifolin bound and unbound Hsp90–cdc37 form. Such analysis showed that the first two eigenvectors account for 21.2% and 16.5% (i.e. 37.7%) of all the motion in taxifolin bound complex while 28.8% and 14.4% (i.e. 43.2%) in case of taxifolin unbound complex (Fig. 11).

In addition, for each snapshot the projection of a trajectory on first and second eigenvector was calculated. Time-development of a conformational change associated with a given eigenvector was compared between taxifolin bound and unbound form. The projection of trajectories on first eigenvector in taxifolin bound and unbound form was found opposite to each other while on second eigenvector showed similarity in projection at different time intervals of the simulation. The probability of sampling the phase space determined by first two principal modes during the simulations of the protein was presented in Figs. 12 and 13. From these figures it is evident that the protein was sampling different conformational space during the simulation. In a recent study Jiang et al.

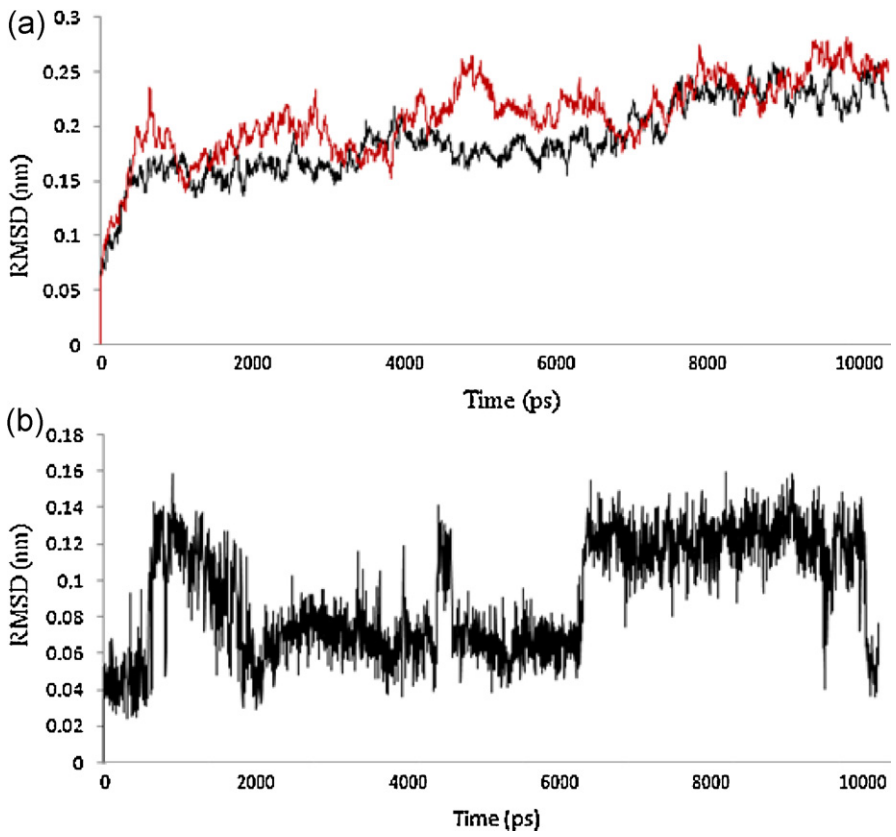

Fig. 6. (a) Plot of root mean square deviation (RMSD) of backbone of Hsp90–cdc37 unbound (black) and Hsp90–cdc37–taxifolin complex (red). (b) Plot of root mean square deviation (RMSD) of taxifolin. (For interpretation of the references to color in this figure legend, the reader is referred to the web version of this article.)

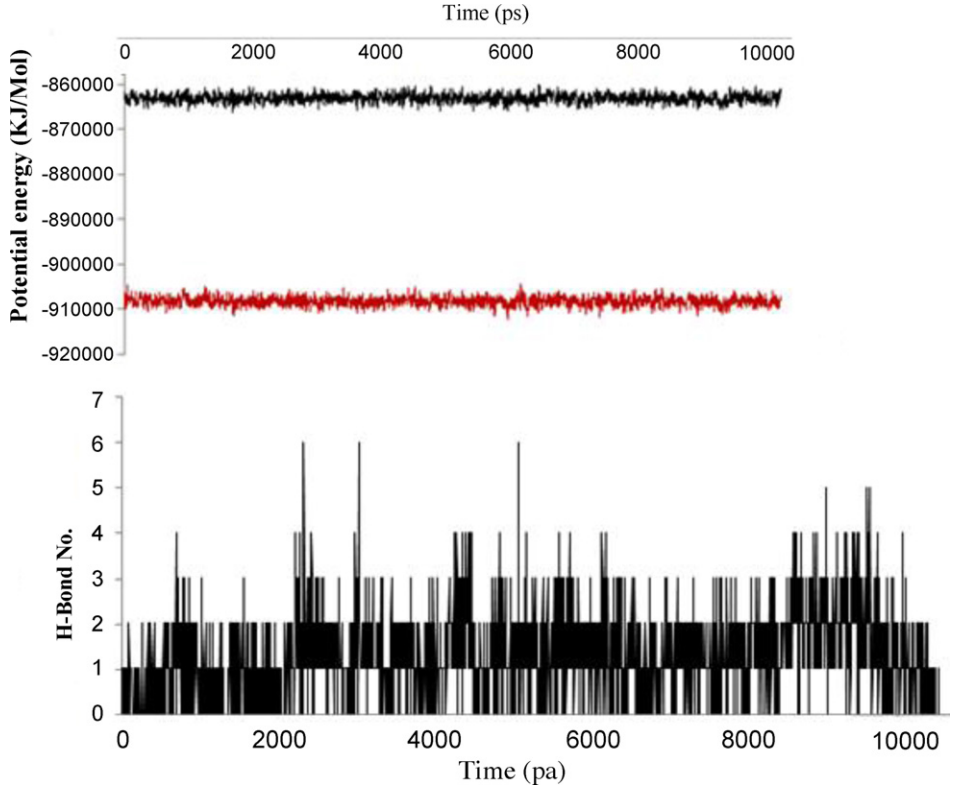

Fig. 7. (a) Potential energy profile of Hsp90–cdc37 unbound (black) and Hsp90–cdc37–taxifolin complex (red) during 10,000 ps MD simulation. (b) Number of H-bonds formed between taxifolin and Hsp90–cdc37 interface residues during 10,000 ps MD simulation. (For interpretation of the references to color in this figure legend, the reader is referred to the web version of this article.)

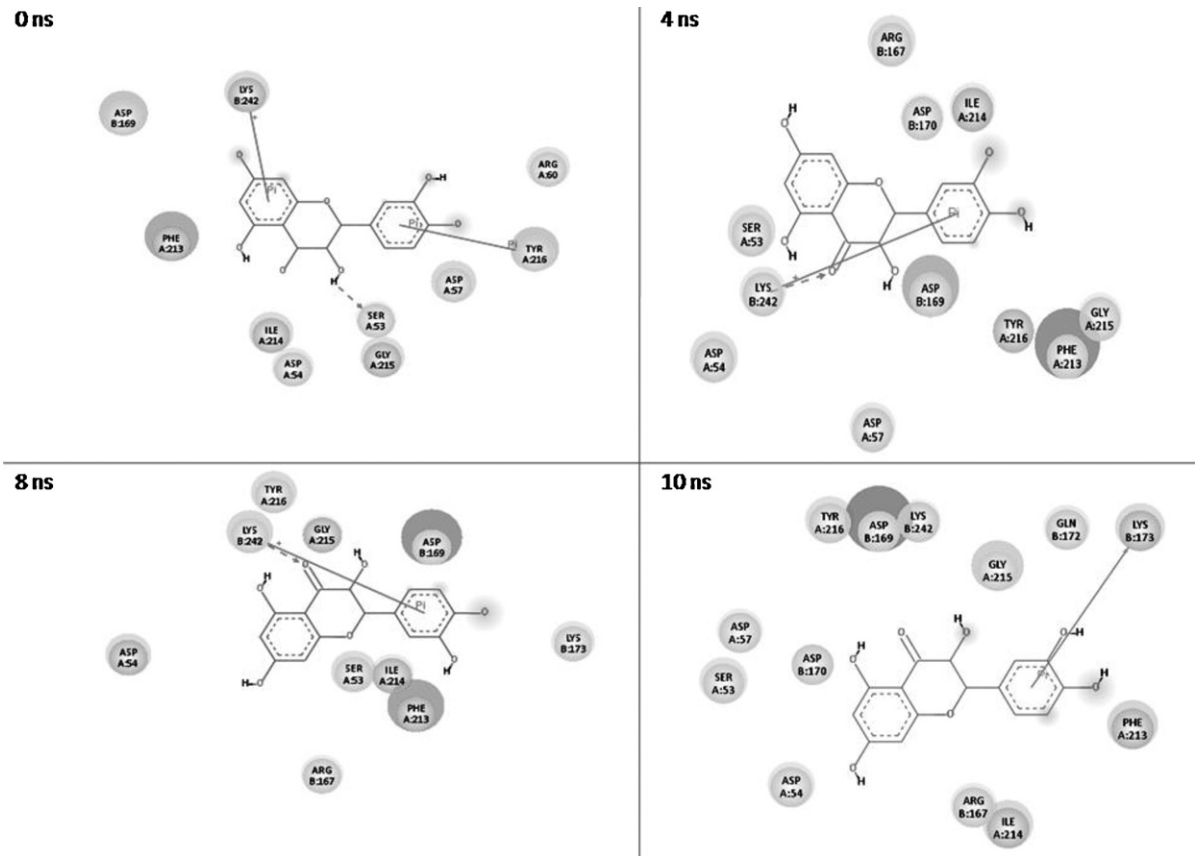

Fig. 8. 2D plots of interaction between taxifolin and Hsp90–cdc37 complex at different time interval of MD simulation.

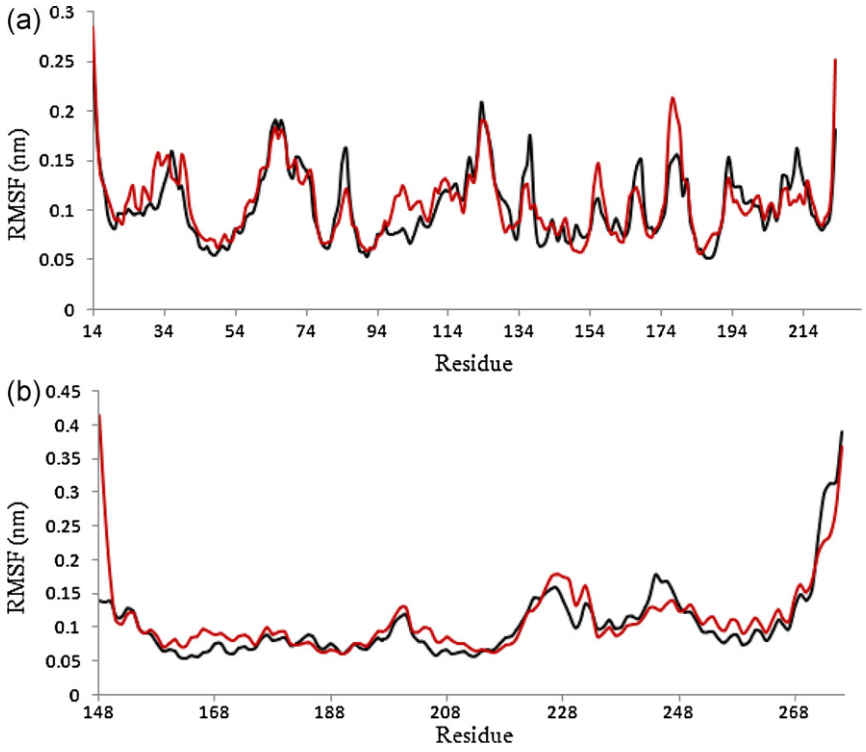

Fig. 9. (a) RMSF of Hsp90 residues backbone (black) in Hsp90–cdc37 complex (taxifolin unbound) and Hsp90 residues backbone (red) in Hsp90–cdc37 complex (taxifolin bound). (b) RMSF of Cdc37 residues backbone (black) in Hsp90–cdc37 complex (taxifolin unbound) and Cdc37 residues backbone (red) in Hsp90–cdc37 complex (taxifolin bound). (For interpretation of the references to color in this figure legend, the reader is referred to the web version of this article.)

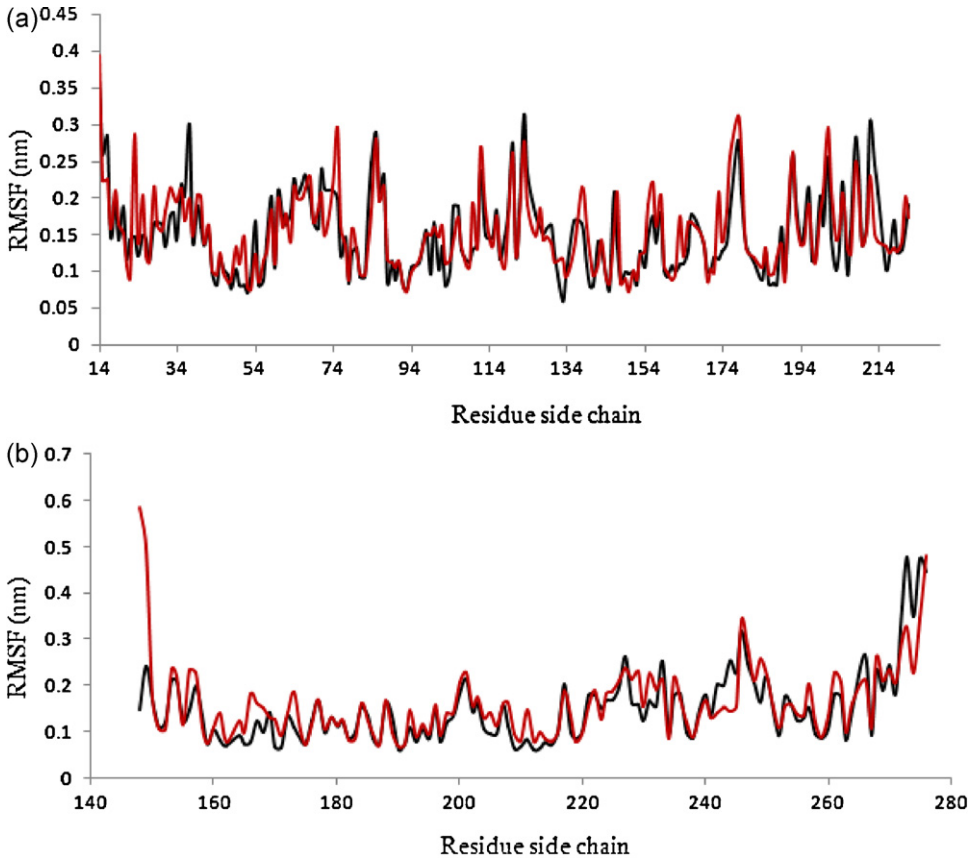

Fig. 10. (a) RMSF of Hsp90 residue side chains (black) in Hsp90–cdc37 complex (taxifolin unbound) and Hsp90 residue side chains (red) in Hsp90–cdc37 complex (taxifolin bound). (b) RMSF of Cdc37 residue side chains (black) in Hsp90–cdc37 complex (taxifolin unbound) and Cdc37 residue side chains (red) in Hsp90–cdc37 complex (taxifolin bound). (For interpretation of the references to color in this figure legend, the reader is referred to the web version of this article.)

reported that mutations in Hsp90 (Q133A, F134A, and A121N) and mutations in Cdc37 (M164A, R167A, L205A, and Q208A) reduced the Hsp90–cdc37 interaction by 70–95% as measured by the resorted luciferase activity through Hsp90–cdc37-assisted complementation [53]. Mutations in Hsp90 (E47A and S113A) and a mutation in Cdc37 (A204E) decreased the Hsp90–cdc37 interaction by 50%. In contrast, mutations of Hsp90 (R46A, S50A, C481A, and C598A) and Cdc37 (C54S, C57S, and C64S) did not change Hsp90–cdc37 interactions [53]. Single amino acid mutation in the interface of Hsp90–cdc37 is sufficient to disrupt the interaction, although Hsp90–cdc37 interactions are through large regions of hydrophobic and polar interactions [53]. These findings revealed the importance of some specific residues critically required for complex formation. During simulation studies we found that

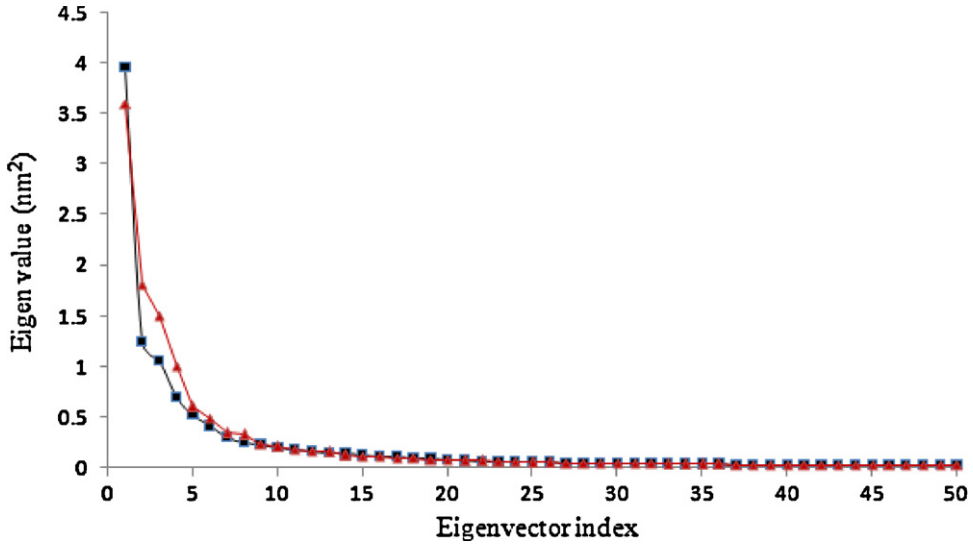

Fig. 11. Eigenvalues of the covariance matrix resulting from the simulations of the Hsp90–cdc37complex (black), Hsp90–cdc37–taxifolin complex (red). (For interpretation of the references to color in this figure legend, the reader is referred to the web version of this article.)

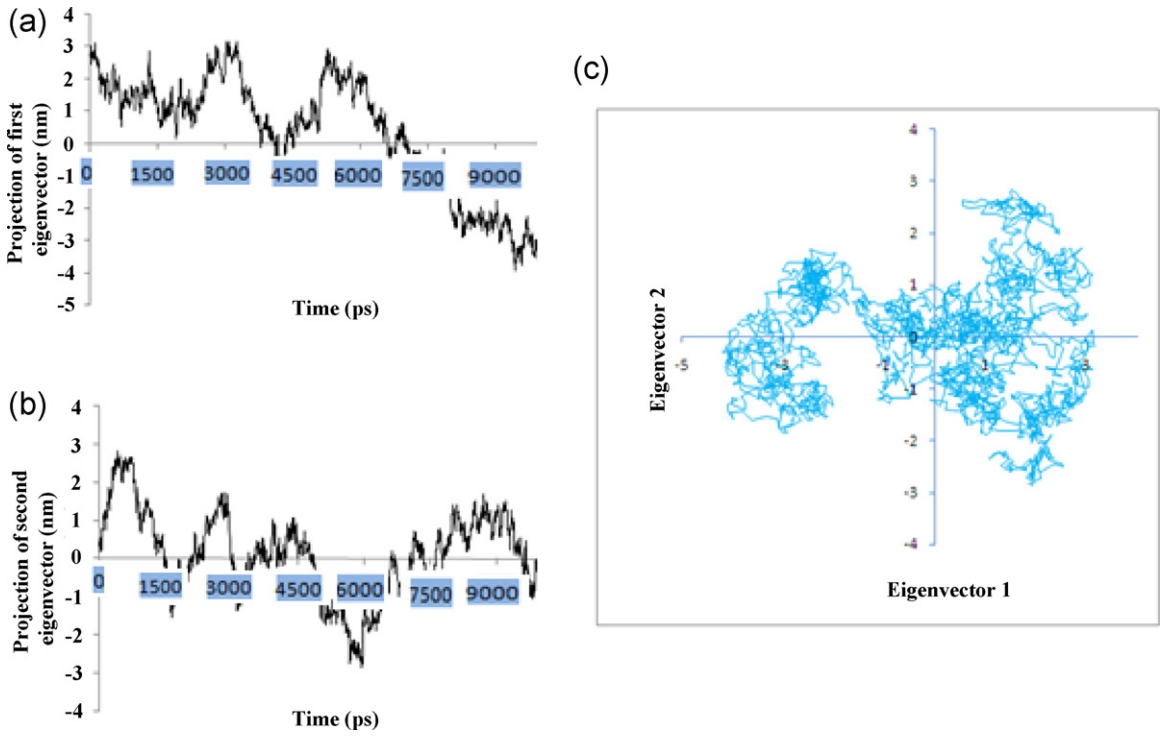

Fig. 12. (a) Projection of the first eigenvector to a trajectory of the Hsp90–cdc37 complex (taxifolin unbound). (b) Projection of the second eigenvector to a trajectory of the Hsp90–cdc37 complex (taxifolin unbound). (c) Correlation of first and second eigenvector.

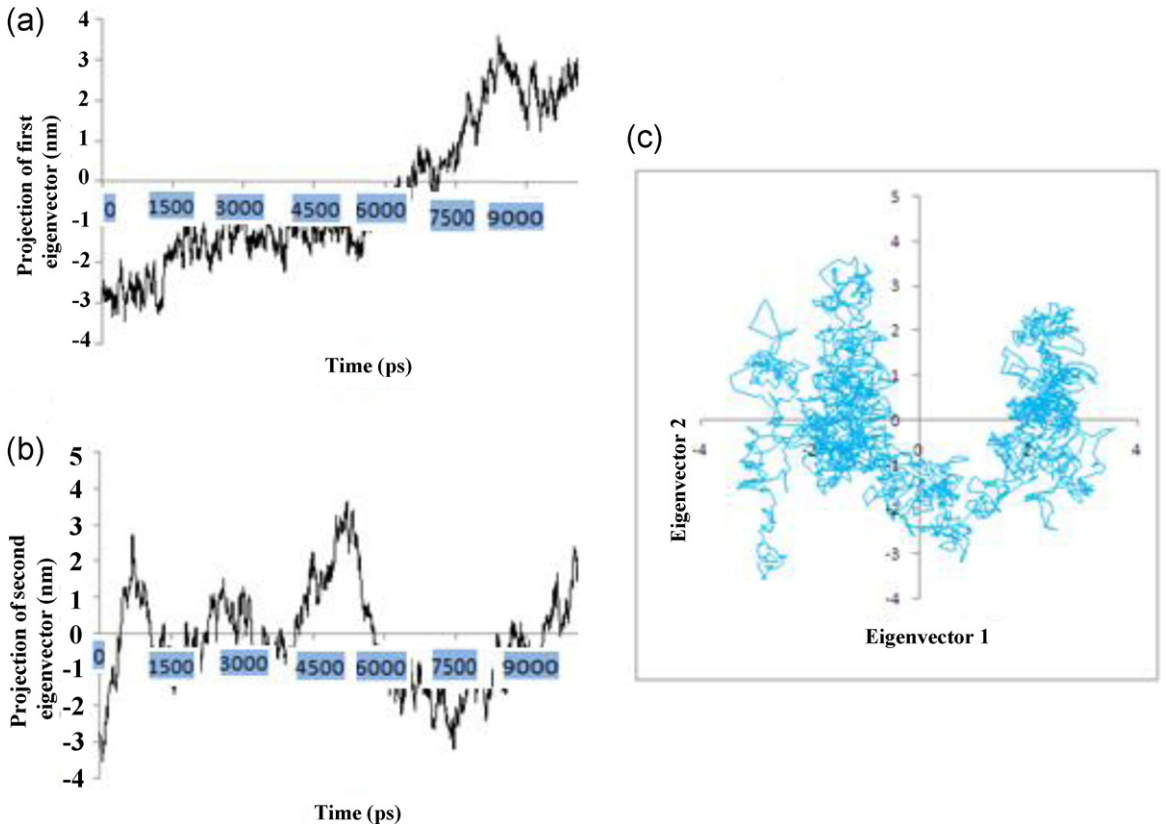

Fig. 13. (a) Projection of the first eigenvector to a trajectory of the Hsp90–cdc37 complex (taxifolin bound). (b) Projection of the second eigenvector to a trajectory of the Hsp90–cdc37 complex (taxifolin bound). (c) Correlation of first and second eigenvector.

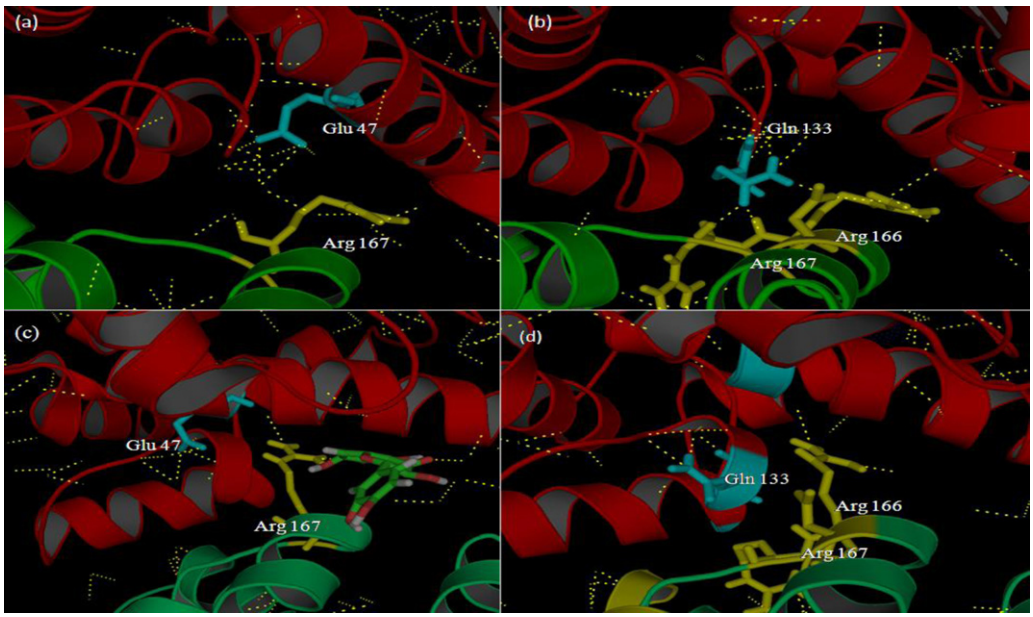

Fig. 14. (a) Interaction between Arg167 of Cdc37 and Glu 47 of Hsp90 in taxifolin unbound form. (b) Interaction between Arg166 and, Arg167 of Cdc37 and Gln133 of Hsp90 in taxifolin unbound form. (c) Disruption of interaction between Arg167 of Cdc37 and Glu 47 of Hsp90 in taxifolin bound form. (d) Disruption of interaction between Arg166 and, Arg167 of Cdc37 and Gln133 of Hsp90 in taxifolin bound form.

taxifolin binding to Hsp90–cdc37 complex disrupt the key interaction required for functional complex formation. A strong interaction between Glu 47 of Hsp90 and Arg167 of Cdc37 bridged by water molecule was vanished in presence of taxifolin (Fig. 14(a) and (c)). Gln 133 of Hsp90 showed polar interaction with Arg166 and Arg167 of Cdc37 during MD simulation of taxifolin unbound form. This interaction significantly contributes to complex formation [53]. Binding of taxifolin to Hsp90–cdc37 complex disrupt this interaction as evidenced by MD simulation (Fig. 14(b) and (d)). A network of polar contact was found Lys 116 and Glu 120 of Hsp90 with peptide bond (—CONH—) of Ala 204 and Leu 205 of Cdc37 (Fig. 15) which was vanished in presence of taxifolin (Fig. 15(a) and (b)). In taxifolin unbound complex Gln 133 of Hsp90 also found to form H-bond with Asp 170 of Cdc37 which was found

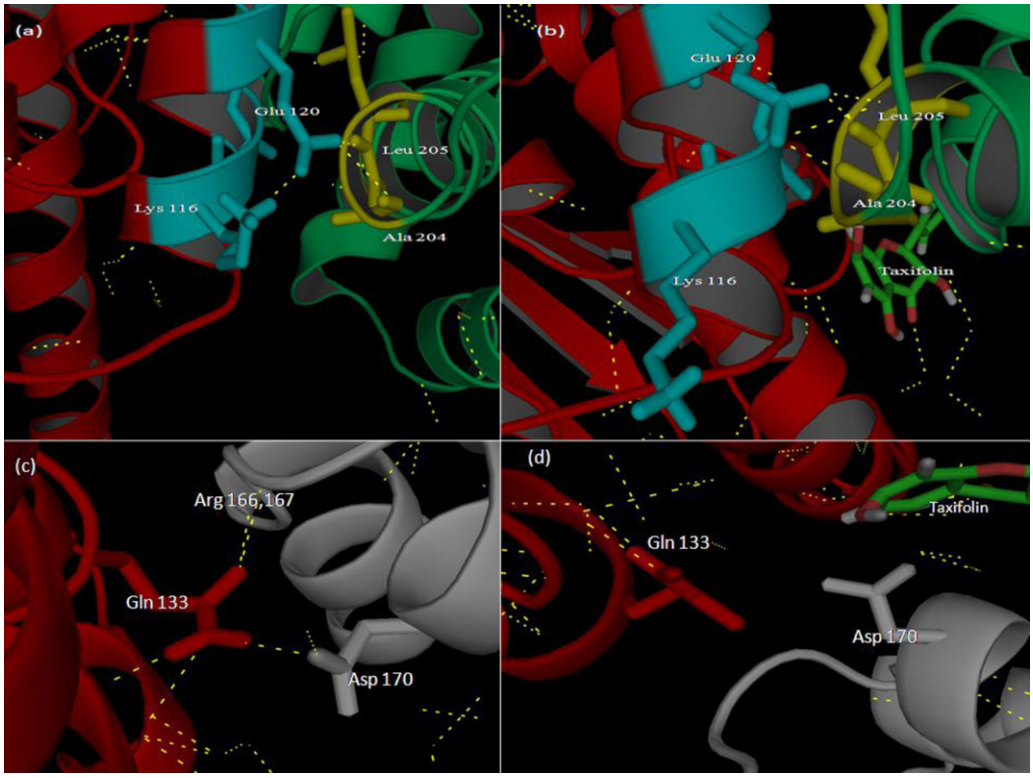

Fig. 15. (a) Interaction between Ala 204, and Leu 205 of Cdc37 and Lys 116, and Glu 120 of Hsp90 in taxifolin unbound form. (b) Interaction between Ala 204 and, Leu 205 of Cdc37 and Lys 116, and Glu 120of Hsp90 in taxifolin bound form. (c) Interaction between Asp 170 of Cdc37 and Gln 133 of Hsp90 in taxifolin unbound form. (d) Disrupted interaction between Asp 170 of Cdc37 and Gln 133 of Hsp90 in taxifolin bound form.

absent in taxifolin bound form (Fig. 15(c) and (d)). These results showed that taxifolin interrupt the residue interaction between Hsp90 and Cdc37 which are critically required for active complex formation. Thus, the taxifolin when bound to ATP binding site of Hsp90 prevented the dimerization by disrupting ATPase cycle. On the other hand, on binding to Hsp90–cdc37 interface, it disrupted the interaction between the interface residues of Hsp90 and Cdc37, which were found to play critical role in the formation of super-chaperone complex.

4. Conclusion

Molecular chaperones perform correct folding of many proteins inside the cell and play a significant role in cancer proliferation. Hsp90 (heat shock protein 90) and Cdc37 complex stabilizes a wide range of mutated and over expressed oncogenic proteins. Taxifolin binds to ATP binding site of Hsp90 and prevent its dimerization by stabilizing open lid conformation which is required for proper functioning. This study significantly contributes to ligand-based modulation of the Hsp90 NTD conformational dynamics and supports the mechanism of the active site lid as a nucleotide sensitive conformational switch. On the other hand, taxifolin interrupts the interaction of interface residues of Hsp90 and Cdc37 complex and provides a novel mechanism for chaperoning process inhibition. The dual action of taxifolin on chaperoning process may lead to significant development of drug candidates to target the folding of oncogenic proteins.

Acknowledgement

One of the authors (Sharad Verma) is thankful of Council of Scientific and Industrial Research (CSIR), India for providing Senior Research Fellowship.

Appendix A. Supplementary data

Supplementary data associated with this article can be found, in the online version, at http://dx.doi.org/10.1016/j.jmgm.2012.04.004.

References

[1] L. Whitesell, S.L. Lindquist, HSP90 and the chaperoning of cancer, Nature Reviews Cancer 5 (2005) 761–772.
[2] L.H. Pearl, Hsp90 and Cdc37 – a chaperone cancer conspiracy, Current Opinion in Genetics & Development 15 (2005) 55–61.
[3] S.K. Calderwood, M.A. Khaleque, D.B. Sawyer, D.R. Ciocca, Heat shock proteins in cancer: chaperones of tumorigenesis, Trends in Biochemical Sciences 31 (2006) 164–172.
[4] M. Ferrarini, S. Heltai, M.R. Zocchi, C. Rugarli, Unusual expression and localization of heat-shock proteins in human tumor-cells, International Journal of Cancer 51 (1992) 613–619.
[5] W.J. Welch, J.R. Feramisco, Purification of the major mammalian heat-shock proteins, Journal of Biological Chemistry 257 (1982) 4949–4959.
[6] A. Kamal, M.F. Boehm, F.J. Burrows, Therapeutic and diagnostic implications of Hsp90 activation, Trends in Molecular Medicine 10 (2004) 283–290.
[7] T. Hunter, R.Y.C. Poon, Cdc37: a protein kinase chaperone, Trends in Cell Biology 7 (1997) 157–161.
[8] C.K. Vaughan, U. Gohlke, F. Sobott, V.M. Good, M.M.U. Ali, C. Prodromou, C.V. Robinson, H.R. Saibil, L.H. Pearl, Structure of an Hsp90–Cdc37–Cdk4 complex, Molecular Cell 23 (2006) 697–707.
[9] A.M. Silverstein, N. Grammatikakis, B.H. Cochran, M. Chinkers, W.B. Pratt, P50 (Cdc37) binds directly to the catalytic domain of Raf as well as to a site on hsp90 that is topologically adjacent to the tetratricopeptide repeat binding site, Journal of Biological Chemistry 273 (1998) 20090–20095.
[10] A. Grover, A. Shandilya, V. Agrawal, P. Pratik, D. Bhasme, V.S. Bisaria, D. Sundar, Blocking the chaperone kinome pathway: mechanistic insights into a novel dual inhibition approach for supra-additive suppression of malignant tumors, Biochemical and Biophysical Research Communications 404 (2011) 498–503.
[11] L.H. Pearl, C. Prodromou, Structure and mechanism of the Hsp90 molecular chaperone machinery, Annual Review of Biochemistry 75 (2006) 271–294.
[12] A. Donnelly, B.S. Blagg, Novobiocin and additional inhibitors of the Hsp90 C-terminal nucleotide-binding pocket, Current Medicinal Chemistry 15 (2008) 2702–2717.
[13] M.M. Ali, S.M. Roe, C.K. Vaughan, P. Meyer, B. Panaretou, P.W. Piper, C. Prodromou, L.H. Pearl, Crystal structure of an Hsp90–nucleotide-p23/Sba1 closed chaperone complex, Nature 440 (2006) 1013–1017.
[14] C. Prodromou, L.H. Pearl, Structure and functional relationships of Hsp90, Current Cancer Drug Targets 3 (2003) 301–323.
[15] N. Wayne, D.N. Bolon, Dimerization of Hsp90 is required for in vivo function, design and analysis of monomers and dimers, Journal of Biological Chemistry 282 (2007) 35386–35395.
[16] J. Trepel, M. Mollapour, G. Giaccone, L. Neckers, Targeting the dynamic HSP90 complex in cancer, Nature Reviews Cancer 10 (2010) 537–549.
[17] Z.H. Huang, G.Z. Fang, Study on purifying arabinogalactan from Larix gmelini Rupr. by column chromatography, Chemistry and Industry of Forest Products 25 (2005) 125–128.
[18] M. Audron, K. Regina, A. Jonas, N. Narimantas, Inhibition of phthalocyanine-sensitized photohemolysis of human erythrocytes polyphenolic antioxidants: description of quantitatives structure–activity relationships, Cancer Letters 157 (2000) 39–44.
[19] Y. Bong-Sik, L. In-Kyoung, K. Jong-Pyung, C. Sung-Hyun, S. Gyu-Seop, Y. Ick-Dong, Lipid peroxidations inhibitory activity of some constituents isolated from the stem bark of Eucalyptus globulus, Archives of Pharmacal Research 23 (2000) 147–150.
[20] Y. Wang, Y. Zu, J. Long, Y. Fu, S. Li, D. Zhang, J. Li, M. Wink, T. Efferth, Enzymatic water extraction of taxifolin from wood sawdust of Larix gmelini (Rupr.) Rupr. and evaluation of its antioxidant activity, Food Chemistry 126 (2011) 1178–1185.
[21] G.M. Morris, D.S. Goodsell, R.S. Halliday, R. Huey, W.E. Hart, R.K. Belew, A.J. Olson, Automated docking using a lamarckian genetic algorithm and empirical binding free energy function, Journal of Computational Chemistry 19 (1998) 1639–1662.
[22] B. Sudhamalla, M. Gokara, N. Ahalawat, D.G. Amooru, R. Subramanyam, Molecular dynamics simulation and binding studies of beta-sitosterol with human serum albumin and its biological relevance, Journal of Physical Chemistry 114 (2010) 9054–9062.
[23] W.L. DeLano, The PyMOL Molecular Graphics System, DeLano Scientific LLC, San Carlos, CA, USA, 2002, http://www.pymol.org.
[24] H.J.C. Berendsen, D. Van der Spoel, R. Van Drunen, GROMACS – a message passing parallel molecular dynamics implementation, Physics Communications 91 (1995) 43–56.
[25] E. Lindah, B. Hess, D. Van der Spoel, Gromacs 3.0: a package for molecular simulation and trajectory analysis, Journal of Molecular Modeling 7 (2001) 306–317.
[26] A.W. Schuttelkopf, D.M.F. van Aalten, PRODRG: a tool for high-throughput crystallography of protein–ligand complexes, Acta Crystallographica 60 (2004) 1355–1363.
[27] W.F. Van Gunsteren, S.R. Billeter, A.A. Eising, P.H. Hunenberger, P.K.H.C. Kruger, A.E. Mark, W.R.P. Scott, I.G. Tironi, Biomolecular Simulation: The GROMOS96 Manual and User Guide, Vdf Hochschulverlag AG, Zurich, 1996.
[28] W.F. Van Gunsteren, X. Daura, A.E. Mark, The GROMOS force field, in: P. Von Rague Schleyer (Ed.), Encyclopedia of Computational Chemistry, vol. 2, Wiley and Sons, Chichester, UK, 1998, pp. 1211–1216.
[29] Accelrys Software Inc., Discovery Studio Modeling Environment, Release 3.1, Accelrys Software Inc., San Diego, 2011.
[30] Y.L. Janin, Heat shock protein 90 inhibitors, a text book example of medicinal chemistry, Journal of Medicinal Chemistry 48 (2005) 7503–7512.
[31] M. Vilenchik, D. Solit, A. Basso, H. Huezo, B. Lucas, H. He, N. Rosen, C. Spampinato, P. Modrich, G. Chiosis, Targeting wide-range oncogenic transformation via PU24FCL, a specific inhibitor of tumor Hsp90, Chemistry and Biology 11 (2004) 787–797.
[32] M.V. Powers, P. Workman, Inhibitors of the heat shock response: biology and pharmacology, FEBS Letters 581 (2007) 3758–3769.
[33] P. Workman, Overview: translating Hsp90 biology into Hsp90 drugs, Current Cancer Drug Targets 3 (2003) 297–300.
[34] J.S. Isaacs, W.P. Xu, L. Neckers, Heat shock protein 90 as a molecular target for cancer therapeutics, Cancer Cell 3 (2003) 213–217.
[35] L. Neckers, S.P. Ivy, Heat shock protein 90, Current Opinion in Oncology 15 (2003) 419–424.
[36] W.M. Obermann, H. Sondermann, A.A. Russo, N.P. Pavletich, F.U. Hartl, In vivo function of Hsp90 is dependent on ATP binding and hydrolysis, Journal of Cell Biology 143 (1998) 901–910.
[37] C.E. Stebbins, A.A. Russo, C. Schneider, N. Rosen, F.U. Hartl, N.P. Pavletich, Crystal structure of Hsp90–geldanamycin complex: targeting of a protein chaperone by an antitumor agent, Cell 89 (1997) 239–250.
[38] A.K. Shiau, S.F. Harris, D.R. Southworth, D.A. Agard, Structural analysis of E-coli hsp90 reveals dramatic nucleotide-dependent conformational rearrangements, Cell 127 (2006) 329–340.
[39] K. Richter, S. Moser, F. Hagn, R. Friedrich, O. Hainzl, M. Heller, S. Schlee, H. Kessler, J. Reinstein, J. Buchner, Intrinsic inhibition of the Hsp90 ATPase activity, Journal of Biological Chemistry 281 (2006) 11301–11311.

[40] G. Colombo, G. Morra, M. Meli, G. Verkhivker, Understanding ligand-based modulation of the Hsp9 molecular chaperone dynamics at atomic resolution, Proceedings of the National Academy of Sciences of the United States of America 105 (2010) 7976–7981.
[41] K. Terasawa, M. Minami, Y. Constantly, Updated knowledge of Hsp90, Journal of Biochemistry 137 (2005) 443–447.
[42] D. Picard, Heat-shock protein 90, a chaperone for folding and regulation, Cellular and Molecular Life Sciences 59 (2002) 1640–1648.
[43] H. Wegele, L. Müller, J. Buchner, Hsp70 and Hsp90 – a relay team for protein folding, Reviews of Physiology Biochemistry and Pharmacology 151 (2004) 1–44.
[44] S.I. Reed, The selection of S. cerevisiae mutants defective in the start event of cell division, Genetics 95 (1980) 561–577.
[45] J.R. Smith, P.A. Clarke, E. de Billy, P. Workman, Silencing the cochaperone CDC37 destabilizes kinase clients and sensitizes cancer cells to HSP90 inhibitors, Oncogene 28 (2009) 157–169.
[46] T. Zhang, A. Hamza, X. Cao, B. Wang, S. Yu, C.G. Zhan, D. Sun, A novel Hsp90 inhibitor to disrupt Hsp90/Cdc37 complex against pancreatic cancer cells, Molecular Cancer Therapeutics 7 (2008) 162–170.
[47] T. Zhang, Y. Li, Y. Yu, P. Zou, Y. Jiang, D. Sun, Characterization of celastrol to inhibit Hsp90 and Cdc37 interaction, Journal of Biological Chemistry 284 (2009) 35381–35399.
[48] M. MacLean, D. Picard, Cdc37 goes beyond Hsp90 and kinases, Cell Stress and Chaperones 8 (2003) 114–119.
[49] J. Shao, A. Irwin, S.D. Hartson, R.L. Matts, Functional dissection of Cdc37: characterization of domain structure and amino acid residues critical for protein kinase binding, Biochemistry 42 (2003) 12577–12588.
[50] S.M. Roe, M.M. Ali, P. Meyer, C.K. Vaughan, B. Panaretou, P.W. Piper, C. Prodromou, L.H. Pearl, The mechanism of Hsp90 regulation by the protein kinase-specific cochaperone p50 (Cdc37), Cell 116 (2004) 87–98.
[51] W. Zhang, M. Hirshberg, S.H. McLaughlin, G.A. Lazar, J.G. Grossmann, P.R. Nielsen, F. Sobott, C.V. Robinson, S.E. Jackson, E.D. Laue, Biochemical and structural studies of the interaction of Cdc37 with Hsp90, Journal of Molecular Biology 340 (2004) 891–907.
[52] S. Sreeramulu, H.R. Jonker, T. Langer, C. Richter, C.R. Lancaster, H. Schwalbe, The human Cdc37.hsp90 complex studied by heteronuclear NMR spectroscopy, Journal of Biological Chemistry 284 (2009) 3885–3896.
[53] Y. Jiang, D. Bernard, Y. Yu, Y. Xie, T. Zhang, Y. Li, J.P. Burnett, X. Fu, S. Wang, D. Sun, Split renilla luciferase protein fragment-assisted complementation (SRL-PFAC) to characterize Hsp90–cdc37 complex and identify critical residues in protein/protein interactions, Journal of Biological Chemistry 285 (2010) 21023–21036.
[54] A. Grover, A. Shandilya, V. Agrawal, P. Pratik, D. Bhasme, V.S. Bisaria, D. Sundar, Hsp90/Cdc37 chaperone/co-chaperone complex, a novel junction anticancer target elucidated by the mode of action of herbal drug Withaferin A, BMC Bioinformatics 12 (Suppl. 1) (2011) S30.
[55] A. Grover, A. Shandilya, V.S. Bisaria, D. Sundar, Probing the anticancer mechanism of prospective herbal drug Withaferin A on mammals: a case study on human and bovine proteasomes, BMC Genomics 11 (Suppl. 4) (2010) S15.
[56] A. Amadei, A.B. Linssen, H.J. Berendsen, Essential dynamics of proteins, Proteins 17 (1993) 412–425.
[57] A. Amadei, A.B. Linssen, B.L. de Groot, D.M. van Aalten, H.J. Berendsen, An efficient method for sampling the essential subspace of proteins, Journal of Biomolecular Structure and Dynamics 13 (1996) 615–625.
[58] H. Yamaguchi, D.M. van Aalten, M. Pinak, A. Furukawa, R. Osman, Essential dynamics of DNA containing a cis·syn cyclobutane thymine dimer lesion, Nucleic Acids Research 26 (1998) 1939–1946.
[59] D.M. van Aalten, J.B. Findlay, A. Amadei, H.J. Berendsen, Essential dynamics of the cellular retinol-binding protein – evidence for ligand-induced conformational changes, Protein Engineering 8 (1995) 1129–1135.
[60] S. Haider, G.N. Parkinson, S. Neidle, Molecular dynamics and principal components analysis of human telomeric quadruplex multimers, Biophysical Journal 95 (2008) 296–311.
[61] M.M. Teeter, D.A. Case, Harmonic and quasiharmonic descriptions of crambin, Journal of Physical Chemistry 94 (1990) 8091–8097.